

THE SELF-FOCUSING FRESNEL-DAMMANN
GRATING AND THE FRESNEL BINARY CGH FOR
COMPACT 2-D LIGHT SPOT ARRAY
GENERATION

D P Godwin, D R Selviah, C D Carey
and J E Midwinter

Department of Electronic and Electrical Engineering,
University College London, UK

INTRODUCTION

As the size and complexity of integrated circuits increases, the speed of such devices becomes limited by the interconnections between individual components. Optical interconnection is a way around this bottleneck, and optical components, instead of wires, can be used to send signals, carried by light beams, around VLSI and WSI circuits. One possibility in this optical régime is to create components capable of generating regular arrays of light spots, which could be used to distribute clock signals (reducing clock skew and cross-talk, Parker (1)), or to address arrays of multi quantum well (MQW) modulators (Parry et al (2)), which would act as optical in/out pins for the microelectronic circuitry. A problem of incorporating optical technology, however, is the small size required of the components, and the difficulties in aligning such components with sub-micron precision. Arrays of microlenses fabricated by various means (Daly et al (3), Frank et al (4)), and computer generated holograms (Feldman and Guest (5)), are two solutions to these problems. In the planar-optic configuration (Jahns and Huang (6)), both optical and electronic components are aligned lithographically on the same plane (fig.1).

This paper is concerned with the holographic approach to array generation, as computer generated holograms can be made effectively to multiplex an array of lenses. This has the advantage that the optical component may be less bulky, and that the uniformity of the image array can be made relatively insensitive to the uniformity of the light illuminating the hologram. One type of hologram, which has been investigated by a number of groups (Dammann (7), Vasara et al (8), Imam et al (9)), is the Dammann grating. This is a binary, far-field, Fourier hologram, which provides a high efficiency and uniformity by optimising the phase profile across the hologram. ((9) achieved a theoretical efficiency of 80.9% using repeated fast Fourier transformation and simulated annealing on an eight phase level grating.) Unfortunately, a standard Dammann grating requires Fourier transform lenses, of focal length, f , to be placed both before and after the grating in order to form a two

dimensional array of spots from a point light source. Such a system must be $4f$ in length and the lenses need to be carefully aligned and rigidly mounted. Promising work with graded refractive index lenses is beginning to address these issues (Kirk et al (10)). In this paper we describe the design of a self-focusing Fresnel-Dammann grating, which is a computer generated hologram and does not make use of any refractive elements. The self-focusing Fresnel-Dammann grating is a combination of both near field Fresnel, and far-field Dammann, holograms and is both a compact array generator and requires no alignment since it is a single optical element.

Another approach to lensless array generation is to make use of Fresnel holograms, which produce an image in the near field without requiring Fourier transformation. However, problems can occur with this type of hologram when large numbers of spots are required in the image plane, leading to undesired, although interesting, results. These are due to the high information density in the hologram plane, the limited resolution of the pixels available to encode the hologram, and interference between the spots in the image plane. This paper presents a Fresnel binary hologram that generates an array of 8×8 spots and overcomes these problems. It was also possible to design such a hologram to operate at an oblique angle of incidence along a slanted axis. Such a hologram is ideal for spot array generation in the compact and robust planar optic configuration (fig.1).

THE SELF-FOCUSING FRESNEL-DAMMANN GRATING

We begin by outlining the considerations which led us to develop the Fresnel-Dammann grating. When light of wavelength, λ , is incident on a screen or transparency which has a periodic transmissivity (of repeat distance, d , of the order of several wavelengths), the diffracted plane waves will travel from the object at angles (θ_n) given by the grating equation:

$$n\lambda = d \sin \theta_n \quad (1)$$

where the diffraction order, n is an integer. If a lens of focal length, f , is placed after the object, these waves are brought to a focus in the focal plane of the lens. (The form of the transmissivity within one period determines the overall intensity envelope of the spots in the focal plane.) The spacing, s , of the diffraction orders in the image is given approximately (because $\sin \theta_1 \approx s / f$ for small θ_1) by:

$$s = f\lambda / d \quad (2)$$

The lens is acting as a Fourier transform element and is converting the angular distribution into a spatial distribution. Such an operation can also be performed by a lens when the lens is placed closely in contact with the periodically transparent object. Although the complex light field in the focal plane of the lens will be multiplied by a quadratic phase factor, the intensity distribution will correctly take the form of the Fourier transform. Now consider what would occur if two such periodic transparencies were placed orthogonally i.e. crossed and placed in contact with the lens. By a similar argument a two-dimensional, albeit non-uniform, regular array of light spots would result. Now, if the object is replaced by a Dammann phase grating and if, instead of a refractive lens, a binary phase Fresnel zone plate (FZP) were used for the focusing, we may imagine a situation in which the FZP is placed right up against the Dammann grating. In this case, the whole structure would generate a regular array of uniform-intensity light spots, of limited extent, in the focal plane of the FZP (due to the nature of the diffraction orders produced by a Dammann grating). This situation is equivalent to one in which the grating and FZP are fused into a single element, such that the total phase shift at any point on the element is equal to the sum of the phase shifts that would have been induced by the combination of the FZP and the grating at that point. In this way, we can make a single element, self-focusing Fresnel-Dammann grating, which requires no alignment.

The self-focusing Fresnel-Dammann grating (SFD) presented in this paper is based on a separable, two dimensional Dammann grating, created using crossing points taken from Morrison (11). The ten crossing points used, defined a grating to give an 8x8 spot array, and the repeat distance, d , for this structure was 101.248 μm in both the x - and y -directions. The crossing points were calculated by Morrison to suppress every even order (including the zeroth), and all orders above the sixteenth. The grating was computer generated as a 3.174 x 3.174 mm array of 2 μm square pixels, and stored as a binary file, each bit representing a pixel (0 for a zero phase change, and 1 for π).

In the same way, a Fresnel zone plate was generated and stored. Its size and resolution were the same as those for the grating, and its focal length, f , was 10 mm (for light of wavelength, λ , 632.8 nm). This zone plate

was used as the Fourier transform lens for the Dammann grating and, because there was a direct 1:1 correspondence between the pixels in the grating and in the zone plate files, the two could be combined directly to form a single optical element. This was done by multiplying the bits of the two binary files in an exclusive-OR fashion, and producing a third binary file of the same size. The exclusive-OR operation corresponds to the combination, modulo 2π , of two binary phase gratings.

When illuminated by a plane wave, the above SFD generates an 8x8 array of spots, separated by 125 μm , at a distance of 10 mm from the SFD plane. This spot spacing is twice that given by eqn. (2), because the Dammann structure used eliminates every even grating order. Another point to consider in the design of the SFD, is the numerical aperture of the Fresnel lens. This must be large enough to image all of the points in the array, and results in the condition that the image array must lie within an area equal to that of the Fresnel lens. This can be used to advantage by choosing the size of the SFD to be just large enough to accommodate the desired output array, and small enough that higher orders of diffraction are suppressed. The SFD pattern can be seen in fig.2, and its output, when illuminated by a plane wave from a HeNe laser, can be seen in fig.3. The SFD used to obtain the output shown in fig.3 was an amplitude and not a phase hologram. The manufacture of a phase hologram would give an output contrast and efficiency rather better than that shown in the figure. A drawback of using a simple binary zone plate to focus the Dammann output, is that the increased efficiency of the grating is lost to the multiple foci of the Fresnel lens. However, combining the grating with a multi-level Fresnel zone plate could, in principle, eliminate this problem. Similarly, multi-level Dammann gratings could be combined with multi-level Fresnel zone plates.

An interesting property of the SFD is the wavelength independence (to first order) of the spot spacing – as the wavelength of the incident light increases, the focal length of the Fresnel zone plate decreases, whilst being compensated by the increased dispersion of the Dammann grating. Now we will present a first order analysis of this effect. If we consider first the construction of the zones in a Fresnel zone plate (fig.4), we can obtain an exact expression for its focal length, f , in terms of the size of the first zone. In fig.4, the phase difference, $\delta\phi$, between the origin and a point a distance, r , from the origin (in the plane of the zone plate) due to a wave emanating from a point source a distance, f , away from this plane, is given by:

$$\delta\phi = k \{ \sqrt{r^2 + f^2} - f \} \quad (3)$$

If R (the size of the first zone) is defined as the value of r when $\delta\phi = \pi$, then we may write f in terms of R :

$$f = (4R^2 - \lambda^2) / 4\lambda \quad (4)$$

Considering now the spots diffracted from a periodic structure with a repeat distance, d , (brought to a focus by a lens of focal length, f , which is positioned against the grating, fig.5), we can see that, from the grating eqn. (1):

$$\sin \theta_n = n\lambda / d \quad (5)$$

and, therefore, that:

$$x_n = f \tan \theta_n = f \{ n\lambda / \sqrt{d^2 - n^2\lambda^2} \} \quad (6)$$

where x_n is the position of the n^{th} order diffracted spot. Combining the properties of the zone plate and the grating, by substituting eqn. (2) into eqn. (4), we can get the following exact expression for the position of the spots in the image plane:

$$x_n = (nR^2 / d) \{ 1 - (\lambda / 2R)^2 \} / \sqrt{1 - (n\lambda / d)^2} \quad (7)$$

Expanding this equation to $O(\lambda^2)$ using the binomial expansion, we get the following approximate expression for x_n , when $n\lambda \ll d$:

$$x_n \approx (nR^2 / d) \{ 1 + \lambda^2 \{ (n^2 / 2d^2) - (1/4R^2) \} \} \quad (8)$$

Provided, in addition, that $\lambda \ll R$, then $x_n \approx (nR^2 / d)$, and the spot spacing is independent of the wavelength, λ . ($R \approx 80 \mu\text{m}$ in our case.) As long as the wavelength-dependent focal plane shifts are not critical, this property of the SFD could be very useful. (From (4), $\delta f / f \approx -\delta\lambda / \lambda$.) For instance, an SFD might be designed to act as a wavelength multiplexed fanout coupler to address fibre-optic bundles.

HIGH FANOUT FRESNEL HOLOGRAMS

Another approach to lensless array generation is to design a suitable Fresnel hologram (Kawai and Kohga (12), Kress and Lee (13)). This can be done simply, by calculating the interference pattern at the hologram plane between waves diverging from the desired input beam and waves converging to the desired image array. In our calculation we ignored the amplitude variations of the interference fringes over the hologram plane, and considered only the phase profile. The phase difference in the hologram plane, $\delta\phi(x,y)$, between reference and image waves was given by:

$$\begin{aligned} \delta\phi(x,y) &= \phi_i(x,y) - \phi_0(x,y) \\ &= \phi_i(x,y) - \tan^{-1} \left\{ \frac{\sum_i \sin \phi_i(x,y)}{\sum_i \cos \phi_i(x,y)} \right\} \quad (9) \end{aligned}$$

where x and y are coordinates in the hologram plane.

and all ϕ s represent phases in the hologram plane; ϕ_i is the phase of the reference beam, ϕ_0 is the phase of the image array taken as a whole, and the ϕ_i are the phases of the individual light spots, i , in the image. The hologram is stored as a binary pattern such that, when $\cos \delta\phi \geq 0$, 1 is stored, and when $\cos \delta\phi < 0$, 0 is stored.

The geometry used in our case may be seen in fig.6. The reference was a point source, situated away from the hologram at twice the hologram's "focal length" ($2f$). The image array was symmetric about an axis through the reference source and the centre of the hologram, and this axis made an angle of θ with the hologram normal. The image was formed at a distance of $2f$ from the hologram. Two holograms were generated, one for an incident angle, θ , of 0° , and the other for an angle of 30° . The latter was used in the planar-optic configuration of fig.1. Both holograms were designed with a pixel size of $2 \mu\text{m}$, and produced an 8×8 array of spots separated by $125 \mu\text{m}$ when illuminated by a plane beam of light. Laser light of wavelength 632.8 nm was used in the 0° case, and a spatially coherent white light source (formed by passing white light through a pinhole) was used for the 30° hologram. The 0° hologram had a focal length of 10 mm , and measured $3.174 \times 3.174 \text{ mm}$, whilst the 30° design had a focal length (at 632.8 nm) of 13.856 mm , measured $2.386 \times 2.066 \text{ mm}$ and was designed for use in glass of refractive index 1.457 .

As mentioned above, high information density in the hologram plane (requiring detail in the hologram finer than the pixel size), and interference between spots in the image plane, can lead to undesirable results in such holograms. To overcome these problems, we adjusted the relative phases of the spots in the image array. This corresponds merely to adding a constant phase term (ϕ_i^0) to each of the ϕ_i in eqn. (9). If the function of the image array depends only on the amplitude of the spots, and not on their phases, we can choose any set of ϕ_i^0 we like, without affecting, in theory, the image produced. In practice, however, our choice of ϕ_i^0 can be very important because each image spot has higher orders of diffraction associated with it, and these interfere with the other image spots. If we arrange for these higher diffraction orders to interfere destructively, we can ensure that the image array is the one we expect. The choice of the ϕ_i^0 also affects the hologram pattern, and should be chosen to ensure that the spatial frequencies in the hologram do not require too high a resolution from the hologram writer. We have chosen two sets of ϕ_i^0 : in the first set, the ϕ_i^0 are such that the phase due to each spot is zero at the origin of the hologram plane, and in the second set, the ϕ_i^0 were randomised. The first choice was arbitrary, and was originally made for convention, so that hologram patterns could be compared. The second choice was made with the express intention of causing destructive interference between the unwanted diffraction orders, thereby

increasing the efficiency of the hologram. The performance of the two sets of ϕ_i^0 for the 0° hologram is compared in fig.7 (as before, amplitude holograms were used, as these were all that were available at the time of writing). As can be seen, the non-random set of ϕ_i^0 is a rather poor choice for an 8x8 array generator (the pattern of 8x8 spots not appearing at all), whilst the randomised ϕ_i^0 allow the hologram to work successfully. Pictures of the holograms themselves may be seen in fig.8. The performance of the 30° amplitude hologram with randomised phases can be seen in fig.9. This was placed in a planar optic configuration (fig. 1) for this experiment and the amplitude hologram was used in reflection.

The dramatic change in hologram performance upon the introduction of a random set of ϕ_i^0 , indicates the possibility of choosing an optimum set which would yield a maximum diffraction efficiency and spot uniformity. This would require the use of repeated Fresnel transforms, and an optimisation algorithm such as simulated annealing (13).

CONCLUSION

We have described the design and demonstrated the performance of two types of lensless array generator. The Self-focusing Fresnel-Dammann grating (SFD), and the Fresnel hologram. The SFD is based on a conventional Dammann grating, but obviates the need for extraneous Fourier forming lenses, by combining the grating with a Fresnel zone plate, in an exclusive-OR fashion. No alignment is required and no bulky or dispersive refractive elements are used. The SFD can be designed to suppress higher diffraction orders, and the spacing of the spots it produces is wavelength independent. The full efficiency of the Dammann design could be restored by combining the grating with a multi-level Fresnel lens. A multi-level Dammann grating could also be used.

The Fresnel hologram can be designed for high fanout, but the design must take into account the phases of the light spots in the image array. We have demonstrated this for an 8x8 fanout element, where a set of random phases in the output gave rise to a satisfactory performance, whilst another set of phases gave an undesired, although interesting, result. It should be possible to optimise these phases to produce a more efficient hologram. We have also demonstrated a 30° slanted axis, random phase design, generating a two dimensional array of 8x8 beams, used in reflection, and operating in a multiple reflection, planar-optic configuration. This type of hologram will be of benefit for compact and rugged optical clock distribution and for optical addressing of modulator arrays on VLSI and WSI circuits.

ACKNOWLEDGEMENTS

This work was funded by the SERC through the UCL Optoelectronic Rolling Grant. Many thanks to Mark Abbott for computer hardware aid and to Rutherford Electron Beam Lithographic Facility for mask fabrication.

REFERENCES

1. Parker, J.W., 1991, *J. Lightwave Technol.*, **9**, 117-119
2. Parry, G., Whitehead, M., Stevens, P., Rivers, A., Barnes, P., Atkinson, D., Roberts, J.S., Button, C., Woodbridge, K. and Roberts, C., 1991, *Physica Scripta*, **T35**, 210-214
3. Daly, D., Stevens, R.F., Hutley, M.C. and Davies, N., 1991, "The manufacture of microlenses by melting photoresist", IOP Short meetings series, 30 May 1991, pp 23-24
4. Frank, M., Kufner, M. and Testorf, M., 1991, *Appl. Opt.*, **30**, 2666-2667
5. Feldman, M.R. and Guest, C.C., 1989, *Optical Engineering*, **28**, 915-921
6. Jahns, J. and Huang, A., 1989, *Appl. Opt.*, **28**, 1602-1605
7. Dammann, H., 1970, *Optik*, **31**, 95-104
8. Vasara, A., Taghizadeh, M.R., Turunen, J., Westerholm, J., Noponen, E., Ichikawa, H., Miller, J.M., Jaakkola, T. and Kuisma, S., 1992, *Appl. Opt.*, **31**, 3320-3336
9. Imam, H., Kirk, A.G., Bird, K.D. and Hall, T.J., 1991, "Design of multiphase level holograms", 3rd international conference on holographic systems, components and applications, 16-18 Sept. 1991, IEE, 166-170
10. Kirk, A.G., Imam, H. and Hall, T.J., 1991, "An efficient holographic interconnect in 0.01 cm³", 3rd international conference on holographic systems, components and applications, 16-18 Sept. 1991, IEE, 161-165
11. Morrison, R.L., 1992, *J. Opt. Soc. Am. A*, **9**, 464-471
12. Kawai, S. and Kohga, Y., 1991, *Japanese J. Appl. Phys.*, **30**, L2101-L2103
13. Kress, B.C. and Lee, S.H., 1993, "Iterative design of computer generated Fresnel holograms for free-space optical interconnections", Optical computing topical meeting, Palm Springs, California, March 16-19, 1993 Technical digest series, volume 7, pp 22-25

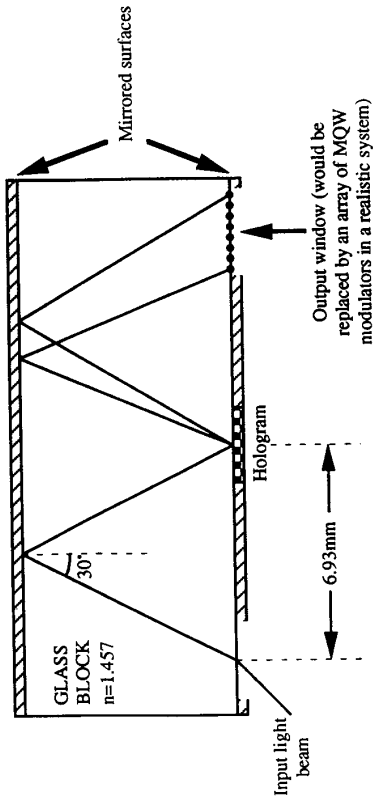


Figure 1: Planar optic configuration

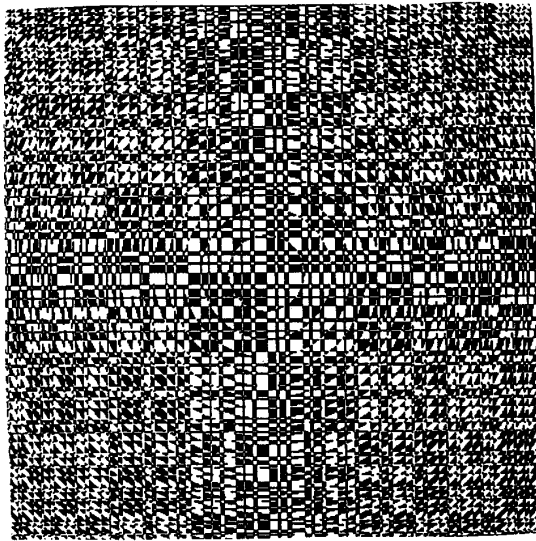


Figure 2: Part of SFD Hologram pattern

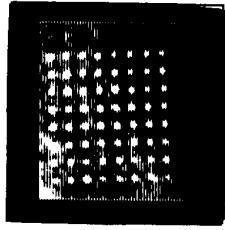


Figure 3: Output of SFD

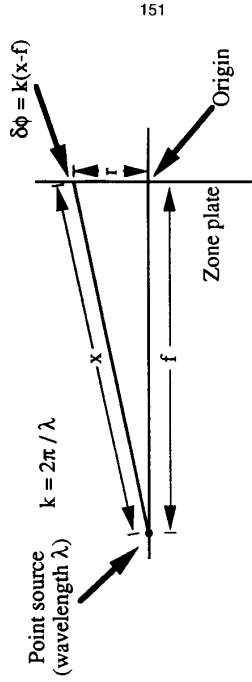


Figure 4: The construction of zones in a Fresnel zone plate

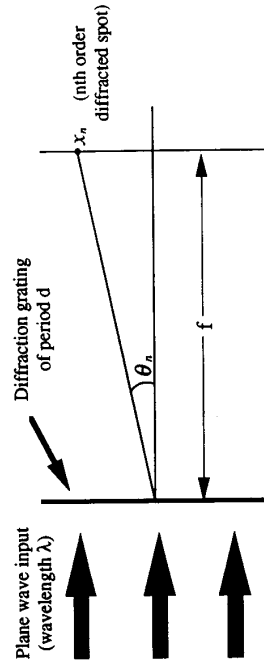


Figure 5: Formation of grating orders

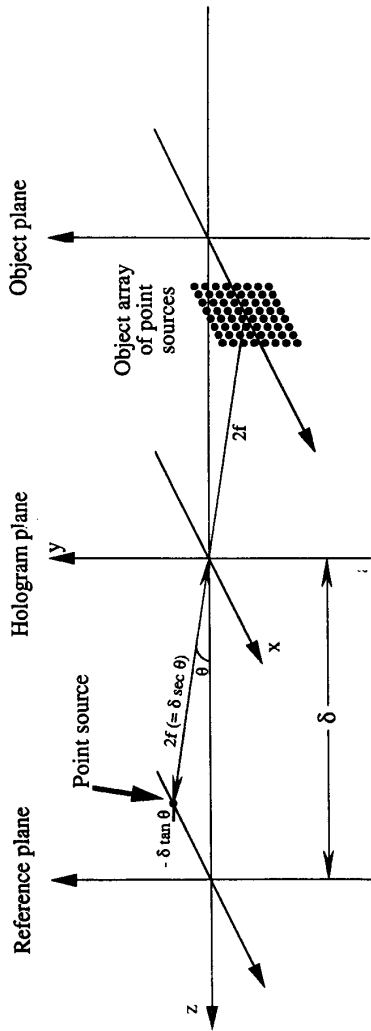


Figure 6: geometry for the generation of a Fresnel hologram

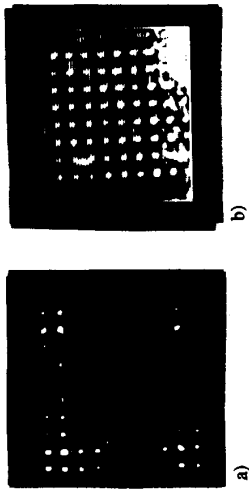


Figure 7: Output of 0° 8x8 Fresnel array generator with
 a) non-random phases
 b) random phases

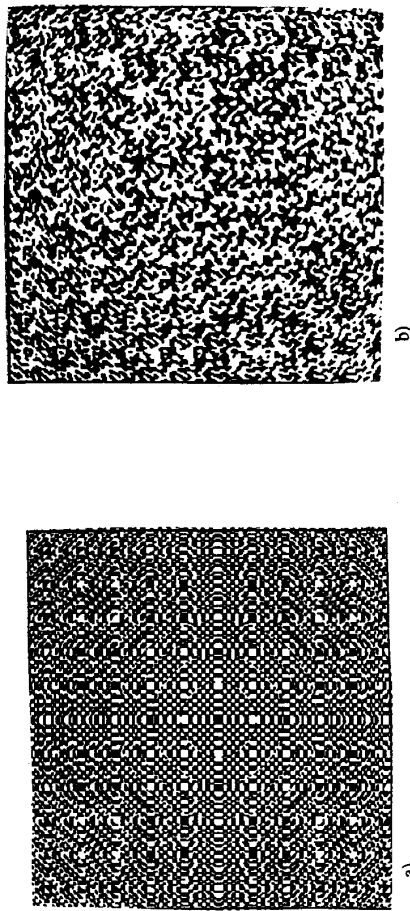


Figure 8: Part of the hologram patterns for the 0° Fresnel array generator with
 a) non-random phases
 b) random phases

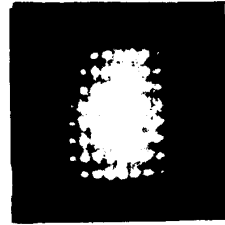


Figure 9: Output of 30° 8x8 Fresnel array generator